RSC Advances

ROYAL SOCIETY OF CHEMISTRY

www.rsc.org/advances

Journal Name

ARTICLE

5-phenyl-dipyrromethane and 5-(4-pyridyl)-dipyrromethane as modular building blocks for bio-inspired conductive molecularly imprinted polymer (cMIP). An Electrochemical and Piezoelectric investigation

Received 00th January 20xx,
Accepted 00th January 20xx

DOI: 10.1039/x0xx00000x

www.rsc.org/

S. Susmel[a§] and C. Comuzzi[b]

5-phenyl-dipyrromethane (5-ph-DP) and 5-(4-pyridyl)dipyrromethane (5-py-DP) are proposed, for the first time, as electroactive building blocks for the preparation of sensors based on molecularly imprinted conductive polymers (cMIP). This paper reports the electrochemical and gravimetric investigation on 5-phenyl-dipyrromethane and 5-(4-pyridyl)dipyrromethane and it demonstrates their ability to form both conductive homo-polymers (cMIP) and co-polymers (co-cMIP). The template salicylic acid (SA) was reversibly and selectively incorporated in the obtained synthetic pockets as confirmed by both voltammetric and piezoelectric investigation. Moreover, the sensitivity of co-cMIP was higher compared to the two homopolymers. The analytical performances confirms that dipyrromethanes, properly functionalized, can be used as electroactive amino acid-like monomers, to prepare bio-inspired imprinted polymers.

Keywords: conductive molecularly imprinted, custom dipyrromethanes, recognition modulation, electrochemical polymerization, salicylic acid.

1.Introduction

The development of sensors based on molecular imprinted polymers (MIP) has received great attention in recent years [1-3]. The preparation of MIP requires that the polymer grows around a template (the target analyte) which is embedded in the polymer network in which it draws a cavity defined by size and stereochemical configuration. Once the template molecule is removed, the cavity acts as a 3D recognition unit highly specific for the target analyte [4]. In order to reach a high level of efficiency for the entire process, it is essential that the template, interacting reversibly with the monomer, does not deactivate its polymerization positions, this holding true especially when the polymerization is electrochemically driven. Pyrrole is frequently used as electroactive monomer for MIP preparation [5, 6]. The template inclusion is driven on the basis of a charge interaction process between the electrogenerated aromatic cation and the template in ionic form. Thus so, the process is poorly versatile and it lacks in selectivity requiring the respect of the above conditions to be efficient [7]. One of the strategies adopted to enlarge the fields of application is to use "bifunctional" monomers whose structures bear both the unit devoted to the molecular recognition and the unit of polymerization. However, in most cases, the functionalization of the monomer impairs its polymerization features, thus solely some molecular structures can be used as recognition moiety. Consequently, the selectivity cannot be accurately tuned. In the present work the electrochemical behaviour of the 5-phenyl-dipyrromethane (5-ph-DP) and 5-(4-pyridyl)-dipyrromethane (5-py-DP)(Figure 1) is investigated, for the first time with the aim to assess whether dipyrromethanes can be useful monomers to synthetize electrochemically conductive MIP (cMIP). The interest in these molecules lies in the fact that the recognition unit is located in a remote position with respect to the two pyrrolic units, which act as polymerization sites. Further, the modular synthesis of dipyrromethanes allows the most convenient functionality for the chemical interaction with the template to be easily introduced in position 5. Then a series of differently

[a] *Department of Food Science, Analytical Chemistry Group, University of Udine, Via Sondrio 2/A-33100 Udine-Italy*
email: sabina.susmel@uniud.it
Tel. +39(0)432 558823 Fax-+39(0)432 558803
§ Corresponding Author

[b] *Department of Chemistry, Physics and Environment, University of Udine, Via del Cotonificio 108-33100 Udine-Italy*
email: clara.comuzzi@uniud.it
Tel. +39(0)432 558845 Fax-+39(0)432 558803
Electronic Supplementary Information (ESI) available: [details of any supplementary information available should be included here]. See DOI: 10.1039/x0xx00000x

substituted dipyrromenthane can be synthetized and conveniently mixed to obtain highly selective cMIP.

In biological receptors, the polypeptidic structure, through the aminoacid-side chains, guarantees the geometrical and chemical complementarity for the specific interaction with ligand. The idea to proof is that a receptor bio-inspired can be reproduced co-polymerising dipyrromethanes differently substituted in C_5. From this perspective, functionalised dipyrromethanes, can be accounted as aminoacid-like electroactive monomers, in which the electrogenerated pyrrolic $\alpha-\alpha$-linkage acts as the peptidic backbone and the substitution in C_5 plays the role of the aminoacid-side chains. The aim of this preliminary study is first to investigate the role of the substituent in 5 both on dipyrromethane polymerization ability and on the recognition of the template. Then, the co-polymerization ability of 5-ph-DP and 5-py-DP is also tested with the goal of demonstrating that multifunctional pockets bearing phenyl and pyridyl pendant groups can be electrochemically obtained. As template prototype of multifunctional ligands the electroactive salicylic acid (SA) [8], was chosen.

The electrochemical investigation of the monomers and their polymerization ability is conducted by cyclic voltammetry (CV) and differential pulse voltammetry (DPV), either in a conventional three-electrode cell and at a Pt-quartz crystal electrode in EQCM (Electrochemical Quartz Crystal Microbalance) device. The simultaneous dual signal of current and mass variation recorded by EQCM is used to investigate the growth of the films at the quartz crystal electrode surface. The obtained MIP-modified crystal was then used in QCM (Quartz Crystal Microbalance) modality to investigate the SA uptake/release by gravimetric signal variation. The selectivity of the piezoelectric quartz crystal (QCM) MIP-modified, is assessed on three interferents, structurally similar to salicylic acid, such as benzoic acid (HBz), phenol (PhOH) and 3-hydroxy-benzoic acid (3-HB). The real samples chosen to test the MIP sensors were the extracts of willow buds. In fact, SA is one of the phytohormones involved in plants adaptive responses to the environmental stresses and it is a key signaling molecule in plant defence against biotrophic pathogens [9,10].

2. Material and methods

2.1. Materials

Salicylic acid (99%) (SA), tetrabutylammonium perchlorate (TBAP), glacial acetic acid (HAc) and acetonitrile (AN) from Sigma-Aldrich (IT) were all of reagent grade.

2.2. Equipment and procedures

2.2.1 Electrochemical investigations

Cyclic voltammetry of 5-ph-DP and 5-py-DP (1 10^{-3} mol L^{-1}) was performed in AN added with 0.05 mol L^{-1} of TBAP at a conventional platinum (Pt) disk working electrode (WE) vs. an $Ag/AgCl,Cl^-_{sat}$ reference electrode and a Pt-foil counter electrode. Before each test, the electrode was carefully cleaned with acetone, than it was mechanically polished with alumina slurry, it was rinsed with Elgastat water (resistivity of 18 MΩcm) and gently dried under a flow of air. The apparent number of electrons exchanged (n_{app}) in the overall process, was obtained from CV data by calculation of the experimental ψ value ($\psi = i_p/A\nu^{1/2}$ c, where the symbols have the usual meaning: i_p = the peak current (A), A = geometrical electrode area (cm^2), ν = scan rate (Vs^{-1}) and c = bulk analyte concentration (M)). n_{app} calculated for 5-ph-DP and 5-py-DP was confirmed by CVs comparison with model compounds such as potassium ferrocyanide ($1e^-$ exchanged) and hydroquinone ($2e^-$ exchanged).

Differential pulse voltammetry (DPV) adopted these optimized conditions: pulse amplitude 50 mV; sample width 20 ms; pulse width 50 ms; pulse period 200 ms; sensitivity 1 10^{-5} AV^{-1}.

All investigations were performed by CHI 400C working station (CH Instruments, Inc., Austin, TX, USA).

2.2.2. Electromicrogravimetric and Microgravimetric investigations

Electromicrogravimetric (EQCM) and Microgravimetric (QCM) investigations of the films were performed at Pt-quartz crystal. Microgravimetric data were obtained measuring the frequency shift due to the mass variation at the quartz surface according to the Saurebray equation [11]:

$$\Delta f = -2f_0^2 \Delta m / [A (\mu\rho)^{1/2}]$$

where Δf is the frequency shift (Hz) due to the added mass, f_0 is the fundamental oscillation frequency of the dry crystal, Δm (g) is the surface mass loading, A is the electrode area, ρ is the density of the crystal, μ is its shear modulus. In the present work, the characteristic of the Pt-quartz crystal used were: AT-cut, f_0 = 8MHz, crystal's density (ρ) 2.684 g/cm^3, shear modulus of quartz (μ) 2.947 x 10^{11}g/cm s^2, electrode area (A) 0.196 cm^2. So, a frequency shift of 1 Hz corresponds to a mass increase of 1.34 ng on the electrode. The quartz crystal, before each use, was polished by 5 min sonication in acetone, 5 min in AN added with 50 % of water solution of soda 0.1 M (prepared in ultrapure water), 5 min in AN added with 1 % of HAc and finally 10 min in ultrapure water. It was gently dried under a flow of air and it was lodged in its Teflon cell (CH Instruments, Inc., Austin, TX, USA). The piezoelectric quartz crystal was connected to CHI 400C working station (CH Instruments, Inc., Austin, TX, USA) to perform the investigations.

2.3. Synthesis of 5-phenyldipyrromethane (5-ph-DP) and 5-(4-pyridyl)-dipyrromethane (5-py-Dp)

5-phenyldipyrromethane (5-ph-DP) and 5-(4-pyridyl)-dipyrromethane (5-py-Dp) were synthesized as reported in literature [12-14]. Briefly, pyrrole (7 ml) and benzaldehyde (0.4 ml) were degassed with N_2 for 15 min. 0.03 ml of trifluoroacetic acid (TFA) were then added and the reaction mixture stirred for 15min. Evaporation to dryness and flash chromatography (Petroleum Ether/Ethyl Acetate 95/5) gave 5-ph-DP in 61 % yield. 4-pyridinecarboxaldehyde (0.9 mL) was stirred for 18 h at 85°C with pyrrole (9.1 mL), under nitrogen atmosphere. Evaporation to dryness and alumina flash-chromatography (Allumina; Ethyl acetate/ Pentane 8/2) afforded 5-py-Dp in 58%.

2.4. NIP and MIP preparation

The polymer deposition was obtained by cycling 17 times the potential between -0.6 V and +1.2 V. This procedure was adopted to obtain both conductive non-imprinted homopolymer (cNIP) and when the tamplate, salicylic acid (SA), was added to the solution, conductive molecularly imprinted homopolymer (cMIP). Monomers were in concentration of 1.0 10^{-3} mol L^{-1} and SA was 1.5 10^{-3} mol L^{-1}. To prepare copolymers (co-cNIP and co-cMIP), different ratio of monomers 5-ph-DP: 5-py-DP =1:2, 1:1, 1:0.5, 1:0.2, 1:0.1 were tested. SA was kept constant at the concentration of 1.5 10^{-3} mol L^{-1} and it was extracted from the imprinted polymers and copolymers by AN added with 1 % HAc (v/v) (about 20 min at RT). The modified electrode was equilibrated 10 min at RT in AN + 0.05 M TBAP before each measurement. These experimental procedures were adopted either in the investigation performed at Pt-working electrode in a conventional three-electrode electrochemical cell either at Pt-quartz crystal electrode for EQCM/QCM investigations.

2.5. QCM evaluation of sensor response

To evaluate the uptake/release of the template by QCM, once the cMIP and co-cMIP were prepared, SA was extracted as procedure in section *2.4 NIP and MIP preparation*. The piezoelectric crystal, which was hold in its Teflon cell, was rinsed with fresh solvent and it was equilibrated with 3 ml of a quiescent solution of AN + 0.05 M TBAP at RT. When the steady frequency was obtained (f_0), SA was added and the variation of the frequency value was monitored to stability (f_1). The signal, Δf, calculated as $\Delta f = f_1 - f_0$ was used to graph the calibration curve vs. SA concentration. A range of SA concentration from 1 10^{-8} mol L^{-1} to 1 10^{-6} mol L^{-1} was investigated. The calculated Δf was also used to obtain ng from Hz, using 1.34 Hz/ng as conversion factor.
The cMIP and co-cMIP selectivity was tested vs 3-hydroxybenzoic acid, phenol and benzoic acid as interferents. To evaluate the aspecific signal of conductive non-imprinted polymer (cNIP) and copolymer (co-cNIP) the same procedures were adopted.

2.6. Real samples

Buds from willows (i.e. *Salix Alba*) were cleaned from scales, frozen with liquid nitrogen than grinded to powder. To extract SA, the procedure optimized was repeated two times on a same sample: 0.10 g of buds powder weight in a Eppendorf vial were added with 1 ml of AN + 1 % HAc (v/v), mixed 60 s on a vortex mixer (ThermoFischer-Scientific-IT) and centrifuged for 10 min at 10,000 G (Centrifuge 5804 R-Eppendorf-DE). The supernatant (1 ml) was transferred to a new vial and the extraction procedure was repeated on the pellet of plant sample. The recovery was assessed on 0.10 g of buds powder spiked with 425 μg of SA. Both the buds powder and the extracted supernatant (2 ml) were stored at - 20°C until use. As reference method, the colorimetric detection (at 540 nm) of the violet-blu complex that SA forms with Fe(III) was used [15].

3. Results and Discussion

3.1. Electrochemical investigation on 5-ph-DP and 5-py-DP and Salicylic acid

The structures of 5-ph-DP and 5-py-DP and their cyclovoltammograms (CV) recorded at Pt-WE are reported in Fig. 1 A and Fig. 1 B, respectively. The potential of the anodic peak (Ep_a) related to the formation of the radical cation was observed, for both monomers, at +1.2 V. A second oxidation process was recorded at +1.5 V for 5-ph-DP and at +1.8 V for 5-py-DP. The apparent number of electrons exchanged (n_{app}) in the first oxidation process was 2.3 e^-/molecule for 5-ph-DP and 1.2 e^-/molecule for 5-py-Dp. Conversely, the ip of second oxidative process of the two dipyrromentanes was comparable. CVs at different scan rate were registered (see Supplementary Information Fig. S1 and Fig. S2) showing that the radical cation was stabilized by the presence of phenyl (ph) group in C5. At 300 mVs^{-1} a quasi-reversible process for 5-ph-DP was observed (reversibility in bipyrrole required a scan rate of 10,000 Vs^{-1}) [16, 17], while, no pseudo-reversibility was observed for 5-py-DP. The basicity of pyridine on the carbocation stability could be responsible of these experimental evidences. Tacking into account the literature reported "pyridine effect" on pyrrole electrochemistry [16- 18, 19-23], the cyclic voltammetry of the N-methylated 5-py-DP derivative was performed. The aim was to ascertained if the halve ip observed in 5-py-DP, respect to 5-ph-DP, was due to a reaction of pyridyl-substituent with the electrogenerated carbocation on dipyrromethane moiety. The quaternization of the pyridine nitrogen causes the displacement of the first oxidation wave toward more anodic potential (data not shown). The i_p of the first oxidation wave was unchanged suggesting that pyridine does not affect the radical cation formation [24, 25], however, i_p of the second process was halving.
CV of 5-py-DP in the presence of tosylate, as stabilizer of radical cation and cationic species through ion-paring [18], was also recorded (see Supplementary Information Fig. S3). It was observed that, increasing the amount of tosylate in solution, i_{pa} of both oxidation processes (at + 1.2 V and + 1.8 V) increased while their Epa became less anodic. Tosylate anion can sterically form ion-pair with $-NH^+$s generated during the oxidation process. The shielding of the positive charge is responsible for the cathodic shift of both oxidation processes. Moreover, i_p related to the radical-cation formation of pyridyl-derivative turns to n_{app}= 2. These data suggest that the low i_{pa} observed (Fig. 1 A and Fig. 1 B) for the first oxidation wave of 5-py-DP is related to the different stability of its radical cation. The effect of pyridil-group is observed just on the process at 1.8 V. On the basis of the mechanism scheme proposed by Zotti el al. [18] for 2,2'-bipyrrole, the hypothesis was formed that pyridine (pKa of pyridine in AN = 16.7 [26]), acting as a H^+ scavenger, drags the reaction toward the product of coupling reaction, helping the deprotonation step necessary for the restoration of conjugation on dipyrromethane [22-25] (Scheme 1 eq. 3) [15-17,22-25].

Scheme 1 near here

The electroactive template was solubilized in acetonitrile (solubility 0.35 M) and its CV profile is reported in Fig. 2 A and Fig. 2 B

together with the voltammetric profile of 5-ph-DP and 5-py-DP. The oxidation of the phenolic group is observed at + 2.1 V, its reduction in the reverse cycle at + 0.6 V, and the cathodic reduction of the carboxylic proton at - 0.5 V. The interactions between monomers and template were investigate recording the first CV cycle separately either in the anodic and the cathodic direction in N_2 bubbled solution. As increasing amounts of SA were added to a 1 mM solution of 5-ph-DP (Fig. 2 A), the oxidation process of -OH increased proportionally, while Epa shifted to more anodic potential suggesting the interaction with the dipyrromethane structure. For 5-py-DP (Fig. 2 B), the SA–OH interaction with the structure of the monomer was much stronger as its oxidation was not visible except when in large excess compared to the concentration of the monomer (at least 4:1). The cathodic part of the cyclovoltamogram of both monomers, showed a less defined reduction process shifted of 150 mV toward more cathodic voltage, indicating the interaction of SA-COOH group with dipyrromethanes.

3.2. Electrochemical investigations of 5-ph-DP and 5-py-Dp cNIP and cMIP. Homo- and co-polymers.

The polymerization ability of both monomers was investigated by EQCM. cNIP and cMIP of homo-and co-polymers formation at Pt-quartz crystal-WE was performed by cyclic voltammetry. The experimental parameters, such as potential limits, scan rate and number of cycles were varied to optimize the film coating. The best potential range was between -0.6 and +1.2 V at a scan rate 0.1 V s^{-1}. During film deposition of homo-5-ph-DP (1 10^{-3} mol L^{-1} in AN + TBAP 0.05M), the current increased progressively and the film formed between + 0.3 V and + 0.4 V giving a cNIP surface coverage (**Γ**) of 3.42 10^{-9} mol cm^{-2} (Fig. 3A). The film thickness increased of 2.7 nm $cycle^{-1}$ showing a linear relation with the cycle numbers as esteemed by profilometry. Also the progressively more negative frequency shift (see Supplementary Information Fig. S4), showed that the film increased regularly its thickness both during the anodic and the reverse scan up to E = 0 V. Then, in the cathodic part of the scan (Ep < 0 V), at each cycle a constant mass release of about 3% was observed. This behavior has been typically observed in conductive polymers with ion exchange capacity, such as polypyrrole [5].

The same conditions were used to polymerize 5-py-DP (1 10^{-3} molL^{-1} in AN + TBAP 0.05 M). In this case cNIP grown at lower potential between - 0.2 V and + 0.2 V (**Γ** = 2.45 10^{-9} mol cm^{-2}) (Fig. 4 A). However, after several cycles the efficiency of deposition process dropped down (mass increases only 0.01% per cycle) (Table 1). The profiles of frequency shift (see Supplementary Information Fig. S5) showed that the mass increase of poly-5-py-DP was confined just to the anodic part of the scan. These evidences suggested that the charge transport in poly-5-py-DP, involving the electrolyte added to the solvent, might be affected by the increasing concentration at the electrode surface of protonated 5-py-DP (see Scheme 1), that finally impairs the film conductivity [22].

Homo-cMIP of both 5-ph-DP and 5-py-DP was formed through the SA inclusion into the polymer network which is thought of occurring through several types of attractive interactions such as π–π interactions between aromatic rings, hydrogen bridges between –OH and –COOH of salicylic acid and N-of dipyrromethane and/ or pyridyl-group in the case of 5-py-DP, charge interactions between the dipyrromethane radical-cation and salicylate in equilibrium with salicylic acid. Homo-cMIPs were prepared using equimolar solution of monomer and template (1mM in AN + 0.05M TBAP) and the same voltage limits and scan rate used in cNIP preparation. CV, DPV and gravimetric data (QCM) were used to demonstrate the inclusion of the template into the films formed and the rebinding ability of the imprinted polymer. The CV of 5-ph-DP cMIP (Fig. 3 B) showed two new peaks compared to the CV of 5-ph-DP cNIP (Fig.3A): the process at -0.4 V, ascribed to the reduction of SA-COOH interacting with 5-ph-DP, and, in oxidation, a new wave at +0.9 V, both rising during deposition. The anodic current at + 1.2 V, at which the radical cation was formed, increased as well during the deposition confirming that the polymer-template interactions do not affect the formation of the radical cation. EQCM measurements clearly confirmed the uptake of SA. Table 1 reports the mass variation at each cycle of film deposition. The mass variation of 5-ph-DP cNIP becomes constant after the second cycle while, for 5-ph-DP cMIP, the mass variation continues to grow indicating the SA uptake. It has to be stressed that both poly-5-ph-DP cNIP and cMIP were conductive during the deposition process suggesting that the inclusion of the electroactive template is not interfering with the polymer growth [27].

The DPV (see Supplementary Information Fig. S4) of 5-ph-DP cNIP and cMIP were also recorded showing a slight difference between the two homo-polymer. Interestingly the DPV of cMIP after washing and re-exposing the sensor to a SA solution, was recovered.

The effect of the numbers of cycles on the extraction of the template from the imprinted polymer was then investigated. The extraction procedure was optimized for a 25 cycles film deposition which traps 2.75 10^{-9} mol cm^{-2} (n = 5, CV % = 10) of SA, as esteemed both by voltammetric and gravimetric data. The best extraction procedure was conditioning the cMIP in AN + TBAP 0.05 M added with 1% (v/v) of acetic acid at open circuit potential for 20 min at room temperature. The solvent acidification increased the SA solubility and helped to break off the interactions established with the polymer matrix.

The inclusion of SA into 5-py-DP polymer was then investigated. The CV of 5-py-DP cMIP (Fig. 3B) shows a growing peak at -0.6 V, again ascribed to the reduction of SA-COOH interacting with the polymer, which is totally absent in the CV of 5-py-DP cNIP (Fig. 3 A). In oxidation however a non-conducting behavior was observed. EQCM measurements of 5-py-DP cMIP deposition (Table 1) shows a loss of the mass variation with the increase of the cycles, due to the dropping of conductivity of the 5-py-DP film. The difference in mass deposition between 5-py-DP cMIP and cNIP is constant at 13.4 ng at each cycle corresponding to a constant uptake of 0.1nmol of SA per cycle. The acidic character of the polymeric structure permanently charged at the protonated pyridin-moiety is considered to influence the diffusion of both the electroactive template and fresh monomer toward the electrode surface [19, 21, 27].

The DPV (see Supplementary Information Fig. S5) of 5-py-DP cNIP and cMIP were also recorded. The non-imprinted polymer was characterized by a double wave (at 1.1 V and 1.6 V) of comparable current density. In the DPV of the imprinted polymer a peak at Ep + 1.4 V was observed whose current density varied when SA was extracted and rebounded to cMIP. The DPVs profiles of both cNIP of

5-ph-DP and 5-py-DP were unchanged after incubation in SA (1 mM) solution. This evidence corroborated that unspecific interactions were not detectable.

Finally, the co-polymer was prepared. The threshold potential for the initiation of polymerization of the two monomers are very close to each other rendering their copolymerization feasible [28-30].

The first scan of the CV of an equimolar (1mM in AN) solution of the two monomers, showed the formation of radical cations as a well-defined peak at + 1.1 V (Fig. 5A). The anticipation of 100 mV of the first oxidation process indicates the interaction between the two monomers. In the following cycles, the evolution of the CV profile with a new oxidation wave at + 0.8 V suggests the formation of a copolymer which increased between + 0.3 V and + 0.5 V. Some features of both homo cNIPs (Fig.3A and Fig. 4A) can be recognized in Fig 5A, i.e. the potential range of film growing and the current intensity are close to the one of 5-ph-DP cNIP. However, the strong indication of the presence of py-derivative in the film is that the deposition, after few cycles becomes less efficient likewise homo-poly-5-py-DP (Table 1). EQCM frequency shift (see Supplementary Information Fig. S6), is affected by the effect of py-derivative as the deposition of co-cNIP was confined to the anodic part of the scans. Interestingly, in the earlier scans, the co-polymer deposits better than homo polymers suggesting a cooperative effect between monomers.

co-cMIP preparation was investigated adding 1.5 mM of SA to a monomer mixture (1mM 5-ph-DP + 1mM 5-ph-DP) (Fig. 5 B). The template inclusion was confirmed by CV where the pre-wave at + 0.9 V is observed as in poly-5-ph-DP (Fig. 3 B). The increment of the cathodic current in the next cycles is also an indication of SA uptake. The SA inclusion was demonstrated by Δf (Hz) variation as the mass deposited at each cycle increased, compared to co-cNIP, of ca. 26 % (Table 1), corresponding to 0.5 nmol cycle^{-1} of SA uptaken.

The Ep and ip observed in DPV of co-cNIP (see Supplementary Information Fig. S6) indicated the presence of both monomers at the modified surface. In co-cMIP the inclusion was suggested by the higher current density of the two oxidation processes at 1.1. V and 1.5 V shifted to slightly more anodic voltage (vs co-cNIP).

Table 2 reports the mass variation after 17 cycles of different monomers feed ratio. It is possible to observe that as the py-monomer concentration increased, the cooperative uptake ability of the MIP increased as well. 5-py-DP enhances SA uptake in co-cMIP participating actively in the binding pocket. Moreover, the extraction time of the template from co-cMIP was doubled respect to homo-phenyl-cMIP due to stronger attractive interactions between pyridyl-moiety and SA. On the other hand, this trend stopped when the concentration of 5-py-DP became prevalent with respect to the concentration of the ph-derivative as a consequence of its interference on the polymerization process [21, 22].

The rebinding ability of co-cMIP was evaluated by QCM (Fig. 6). Co-cMIP prepared from a 1:1 monomer feed ratio shows the best rebinding performances and it was then chosen as sensor for the analytical characterization.

3.3. QCM evaluation of sensor response

The sensor response was evaluated by QCM. The 3D-structure of the cavity left into the polymeric structure is able to rebind selectively the SA added in solution as analyte. A typical trend of the frequency shift observed during the SA rebinding studies at co-cMIP is reported in Fig. 7 . The addition of different concentrations of SA produced an immediate variation of the crystal oscillation frequency and the response time evaluated at 90 % of Δf was ca. 50 s for all cMIP. The template removal from co-cMIP restored the initial Hz value.

The rebinding ability of homo and co-cMIPs prepared from different monomer feed ratio is reported in Fig. 8 as Δf vs concentration of SA (M) added in solution. All cMIP considered showed a dynamic range between 10^{-8} M and 10^{-6} M of SA while the linear range is observed between 10^{-8} M and 10^{-7} M. The detection limits calculated as $3\sigma/S$ were reported in Table 3. Before the SA addition, cMIP was left to equilibrate in solvent. Once the frequency shift was stabilised, the scattering (ΔHz) recorded during 60 s was used to estimate the standard deviation (σ) of the signal.

Poly-5-py-DP gives the lower response in trend with its low polymerization ability with a maximum shift of ca -100 Hz (cv = 18%, n = 3) while poly-5-ph-DP rebinds almost the double of SA. The synergic effect of co-polymers is evidenced in Table 3 where the sensitivity of detection obtained with polymers of different composition is compared. A higher MIP response is produced rising the amount of py derivative in the feed ratio confirming that the monomers feed ratio affects the concentration of the rebinding sites in the imprinted film, modulating its recognition properties. This synergic effect is the result of combining the better polymerization efficiency of 5-ph-DP and the stronger interaction between the SA and the 5-py-DP. The aspecific interations with non-imprinted polymer was evaluated exposing c-NIP and co-cNIP to different SA concentrations (Fig. 8). In all the cNIP the higher shift recorded was ca. - 80 Hz irrespective of the variation of the SA concentration.

Compounds structurally similar to SA, such as 3-hydroxy benzoic acid (3-HB), phenol (PhOH) and benzoic acid (HBz), were selected to test the selectivity of the co-cMIP sensor. co-cMIP was exposed to a 3 10^{-7} mol L^{-1} solution of interferent. Results shown in Fig. 9 highlights that a selective response was obtained. The sensor uptakes PhOH and HBz in comparable amounts suggesting that both the hydroxyl and the carboxylic functions are involved in the network of non-covalent interactions established inside the recognition pocket. However when these two functions are present on the same molecule but in a different position respect to the template, as in 3-HB, the sensor response decreased by a half. Consequently co-cMIP shown the higher selectivity vs. 3-HB, the meta isomer of SA. The data confirm that the geometric fitting, beside the non-covalent interactions, between substrate and co-cMIP recognition pocket is a key factor in determining the sensor performances in term of response and selectivity. These different behaviors demonstrate also that a pocket was obtained. In the hypothesis of an interaction to the surface due to copolymerized pyridine-moiety, it is believed that not obvious differences in the signal provided by the analysed interferents would been seen.

3.4. Co-cMIP tests in real samples

Finally, the SA extracted from spiked buds was esteemed by colorimetric approach (0.0135 mol L^{-1}; recovery of 88%) [10]. The optimized extraction was performed in AN containing acetic acid. The 1% (v/v) of HAc gives both the best extraction performances and the advantage of using the extraction solvent without further manipulation except the dilution. In fact, to avoid saturation of the polymeric film, a concentration of 3 10^{-7} mol L^{-1} of the extract was added to the QCM-co-cMIP and QCM-co-cNIP modified surfaces. On the basis of the measured Δf, an SA concentration of 2.26 10^{-7} mol L^{-1} was esteemed by co-cMIP (recovery of 75%; cv = 11%; n = 3,) and co-cNIP measured an aspecific signal of 7.31 10^{-8} mol L^{-1} (cv = 14%; n = 3).

Conclusions

The monomers 5–ph-DP and 5–py-DP are interesting bifunctional monomers for cMIP construction thanks to the substituent in 5 which interacts with the template during film formation. In the copolymerized MIP a synergistic effect of the monomers was observed so during the rebinding tests an increased sensitivity was measured respect to those obtained when the monomers were individually polymerized. However, more insight would be posed on the role of the py-derivative on the polymerization of the copolymer. This especially because py-moiety is able to establish attractive interactions with a wide range of organic and inorganic compounds. Moreover, these first evidences seem to strongly support our idea that a family of dipyrromethane differently functionalized in C_5 can be synthetized and conveniently used to tune the recognition ability of the cMIP toward the template.

References

1 Y. Lattach, P. Archirel, S. Remita, *J. Phys Chem. B*. 2012, **116**, 1467.
2 F. Aboufazeli, H.R.L.Z Zhad, O. Sadeghi, M. Karimi, E. Najafi, *J. of AOAC Int*., 2014, **97**, 173.
3 L. Uzun, A.P.F.Turner, *Biosens. & Bioelectron., 2015, in press*
4 Songjun Li, Yi Ge, S.A. Piletsky, Joe Lunec, *Molecularly Imprinted Sensors*, Elsevier, Amsterdam, 1st edn, 2012
5 A. Mehdinia, M. O. A. Zanjani, M. Ahmadifar, A. Jabbari, *Biosens. & Bioelectron.* 2013, **39**, 88.
6 S. P. Ozkorucuklu, Y. Sahin, G. Alsancak, *Sensors*, 2008, **8**, 8463.
7 M.J. Whitcombe, I. Chianella, L. Larcombe, S.A. Piletsky, J. Noble, R. Porter, A. Horgan, *Chem. Soc. Rev*., 2011, **40**, 1547.
8 A. Torriero, J.M. Luco, L. Sereno, J. Raba, *Talanta*, 2004, **62**, 247.
9 M. Ashraf, N.A. Akram, R.N. Arteca, M.R. Fooland, *Critical Rew. In Plant Sciences*, 2010, **29**, 162.
10 G. Marek, R. Carver, Y. Ding, E. Sathyanarayan, X. Zhang, Z. Mou, *Plant Methods*, 2010, **6**, 21
11 G.Z. Sauerbay, Phys. 1959, **155**, 206
12 J. W. Ka, C. H. Lee, *Tetrahedron Lett.*, 2000, **41**, 4609.
13 R. P. Briñas, C. Brückner, *Synlett.* 2001, **3**, 442.
14 B. J. Littler, Y. Ciringh, J.S. Lindsey, *J. Org. Chem.,* 1999, **64**, 2864.
15 C.S. Warrier, M. Paul, M.V. Vineetha, *Genetics plant phys*., 2013, **3**, 90.
16 G. Bidan, M. Guglielmi, *Synth. Met*., 1986, **15**, 49.
17 L. Guyard, P. Hapiot, P. Neta, *J. Phys. Chem. B*., 1997, **101**, 5698.
18 G. Zotti, G. Schiavon, S. Zecchin, F. Sannicolò, E. Brenna, *Chem. Mater.*, 1995, **7**, 1464.
19 C.P. Andreiux, P. Audebert, P. Hapiot, J. Saveant, *Synth. Met*., 1991, **41**, 2877.
20 R.J. Waltman, J. Bargon, *Can. J. Chem.,* 1986, **64**, 76.
21 M.G. Cross, D. Walton, J. Morse, R.J. Mortimer, D.R. Rosseinsky, D.J. Simmonds, *J. Electroanal. Chem.,* 1985, **189**, 389.
22 P. N. Bartlett, I.-Y. Chung, P. Moore*, Electrochim. Acta*., 1990, **35**, 1273.
23 A.F. Diaz, A. Martinez, K.K. Kanazawa, *J. Electroanal. Chem.*, 1981, **130**, 181.
24 G.R. Mitchell, F.J. Davis, C.H.E. Legge, *Synth. Met*., 1988, **26**, 247.
25 K.J. Wynne, G.B. Street, *Macromolecules*, 1985, **18**, 2361.
26 F. Eckert, I. Leito, I. Kaljurand, A. Kutt, A. Klamt, M. Deidenhofen, *J. Comp. Chem*., 2009, **30**, 799.
27 L. Özcan, Y.Şahin, *Sensor Actuat. B-Chem*., 2007, **127**, 362.
28 K. Dhanalakshmi, R. Saraswathi, *J. Mat. Sci.*, 2001, **36**, 4107.
29 K.K. Kanazawa, A**.**F. Diaz, M.T. Krounbi, G.B. Street, *Syn. Met*., 1981, **4**, 119.
30 S. Kuwabata, S. Ito, H. Yoneyama, *J. Electrochem. Soc*., 1988, **135** 1691.

Journal Name

ARTICLE

5-phenyl-dipyrromethane and 5-(4-pyridyl)-dipyrromethane as modular building blocks for bio-inspired conductive molecularly imprinted polymer (cMIP). An Electrochemical and Piezoelectric investigation

Received 00th January 20xx,
Accepted 00th January 20xx

DOI: 10.1039/x0xx00000x

www.rsc.org/

S. Susmel[a§] and C. Comuzzi[b]

Figures, Scheme and Tables

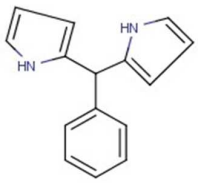

5-phenyl-dipyrromethane (5-ph-DP)

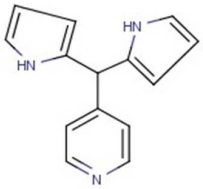

5-(4-pyridyl)-dipyrromethane (5-py-DP)

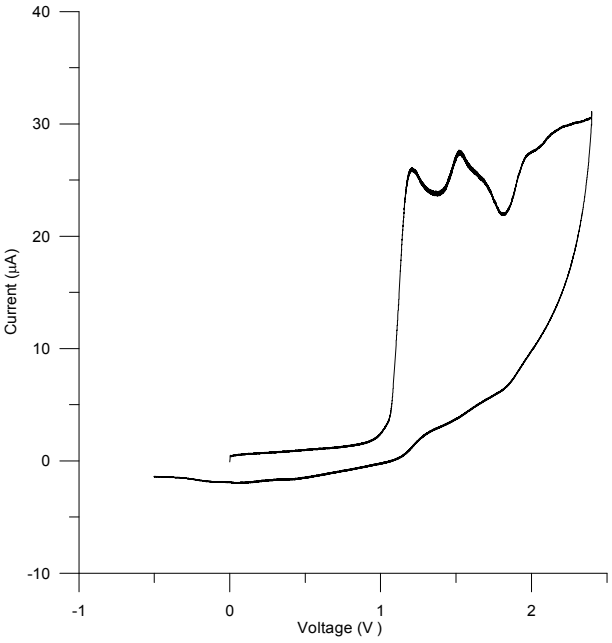

Figure 1 A: structure and cyclovoltammogram of 5-ph-DP 1 mM in AN + 0.05 M TBAP; Pt-WE vs. Ag/AgCl,Cl^-_{sat} ; scan rate 0.10 V s^{-1}.

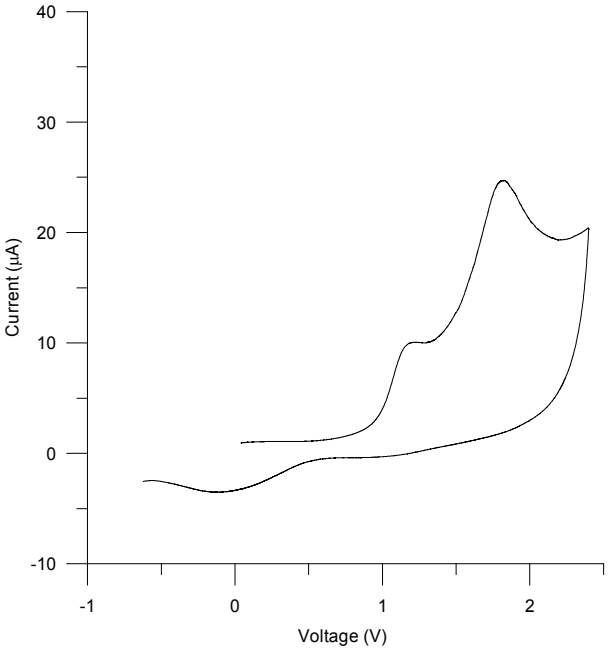

Figure 1 B: structure and cyclovoltammogram of 5-py-DP 1 mM in AN + 0.05 M TBAP; Pt-WE vs. Ag/AgCl,Cl^-_{sat} ; scan rate 0.10 V s^{-1}.

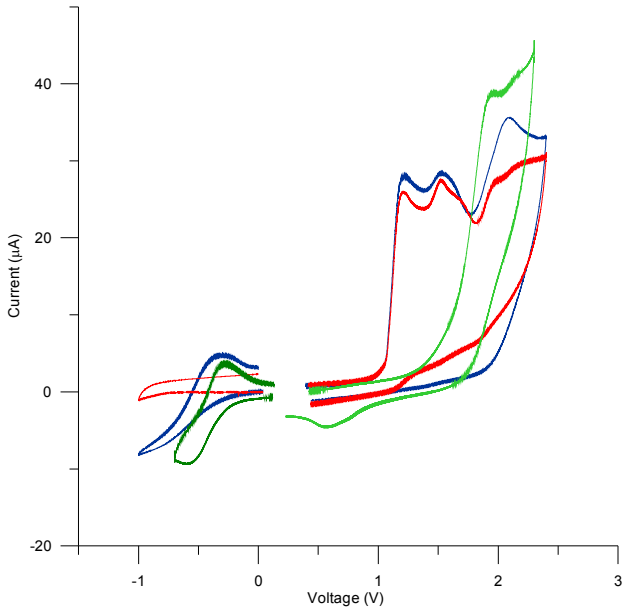

Figure 2 A: anodic and cathodic behaviour of SA 2.5 mM (green line), 5-ph-DP (red line) 1 mM and of 5-ph-DP 1 mM added with SA 1 mM (blue line). CVs recorded at Pt WE vs. Ag/AgCl, Cl^-_{sat} in AN + 0.05 M TBAP; scan rate 0.10 Vs^{-1}

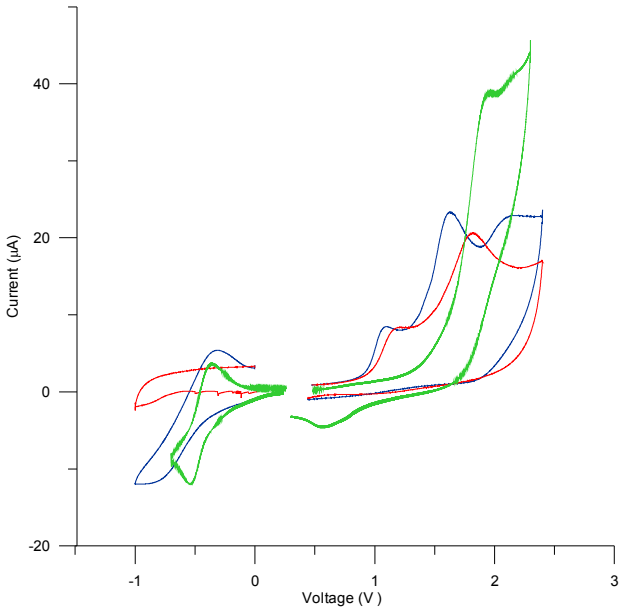

Figure 2 B: anodic and cathodic behaviour of SA 2.5 mM (green line), 5-py-DP (red line) 1 mM and of 5-py-DP 1 mM added with SA 4 mM (blue line). CVs recorded at Pt WE vs. Ag/AgCl, Cl^-_{sat} in AN + 0.05 M TBAP; scan rate 0.10 Vs^{-1}

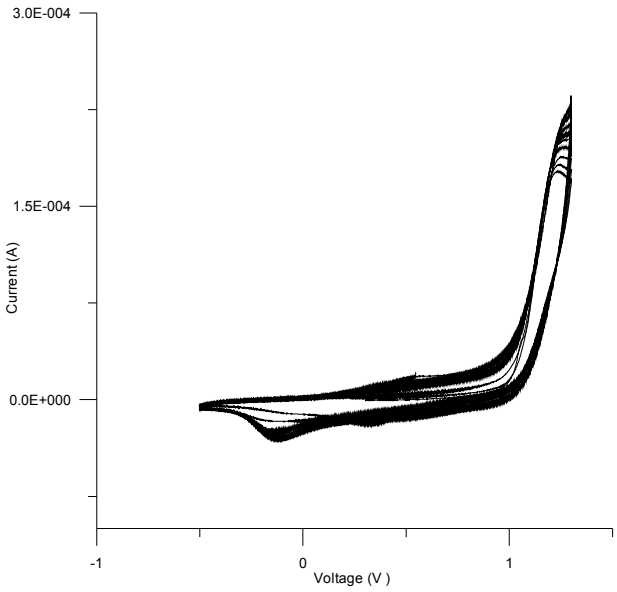

Figure 3 A: deposition by cyclic voltammetry of homo-poly-5-ph-DP (cNIP); [5-ph-DP] = 1 mM. Pt-quartz crystal WE vs. Ag/AgCl, Cl-sat in AN + 0.05 M TBAP; scan rate 0.10 Vs^{-1}.

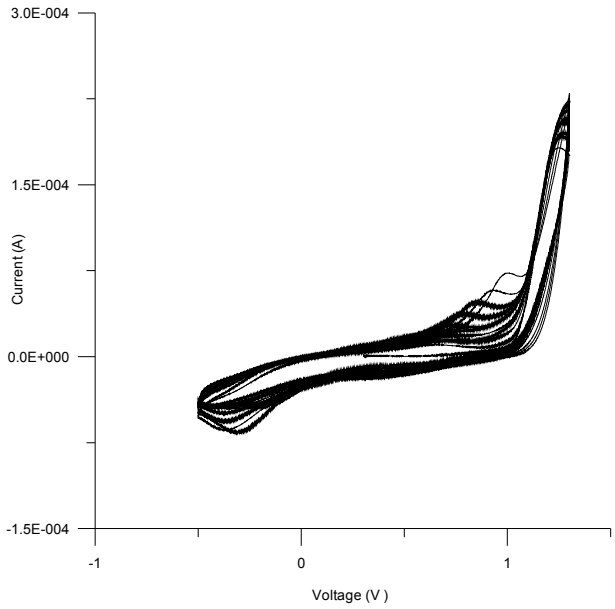

Figure 3 B: deposition by cyclic voltammetry of cMIP; [5-ph-DP] = [SA] = 1 mM. Pt-quartz crystal WE vs. Ag/AgCl, Cl^-_{sat} in AN + 0.05 M TBAP; scan rate 0.10 Vs^{-1}.

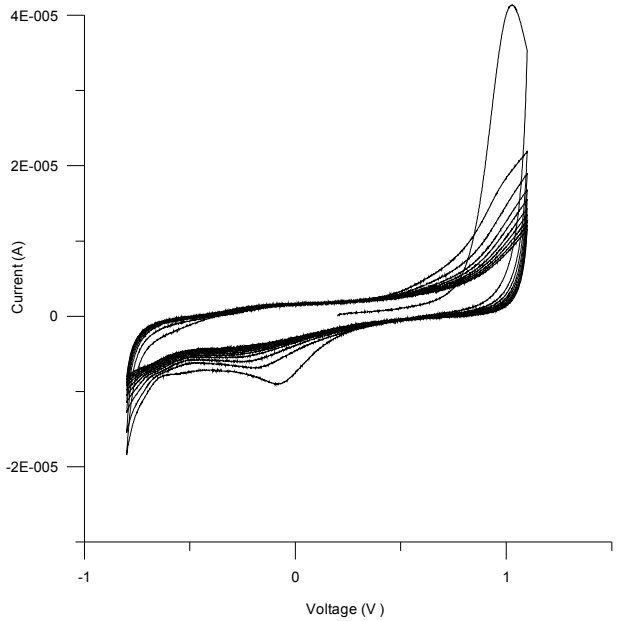

Figure 4 A: deposition by cyclic voltammetry of homo-poly-5-py-DP (cNIP); [5-py-DP] = 1 mM. Pt-quartz crystal WE vs. Ag/AgCl, Cl^-_{sat} in AN + 0.05 M TBAP; scan rate 0.10 Vs^{-1}.

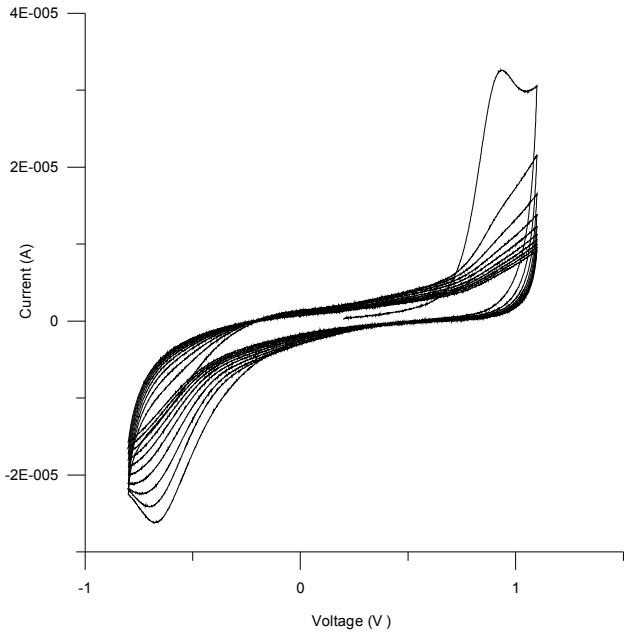

Figure 4 B: deposition by cyclic voltammetry of cMIP; [5-py-DP] = [SA] = 1 mM. Pt-quartz crystal WE vs. Ag/AgCl, Cl^-_{sat} in AN + 0.05 M TBAP; scan rate 0.10 Vs^{-1}.

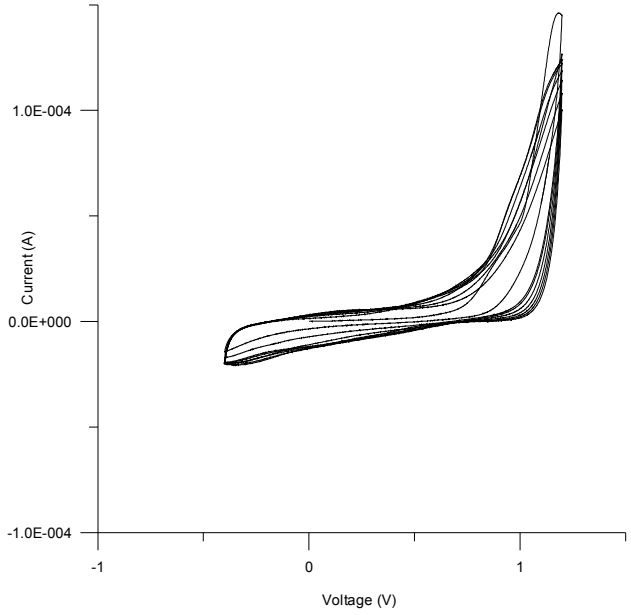

Figure 5 A: CV deposition of co-polymer of 5-ph-DP + 5-py-DP (cNIP), both monomers 1 mM. Pt-quartz crystal WE vs. Ag/AgCl, Cl^-_{sat} in AN + 0.05 M TBAP; scan rate 0.10 Vs^{-1}.

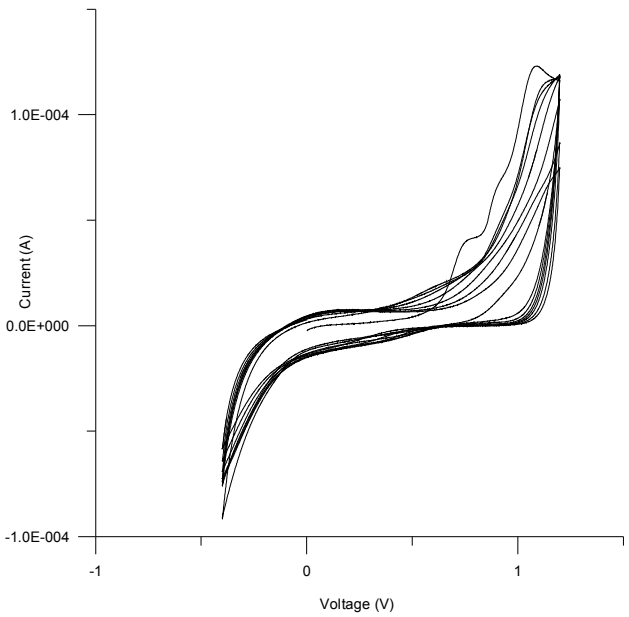

Figure 5 B: CV deposition of co-cMIP, both monomers 1 mM, SA 1.5 mM. Pt-quartz crystal WE vs. Ag/AgCl, Cl^-_{sat} in AN + 0.05 M TBAP; scan rate 0.10 Vs^{-1}.

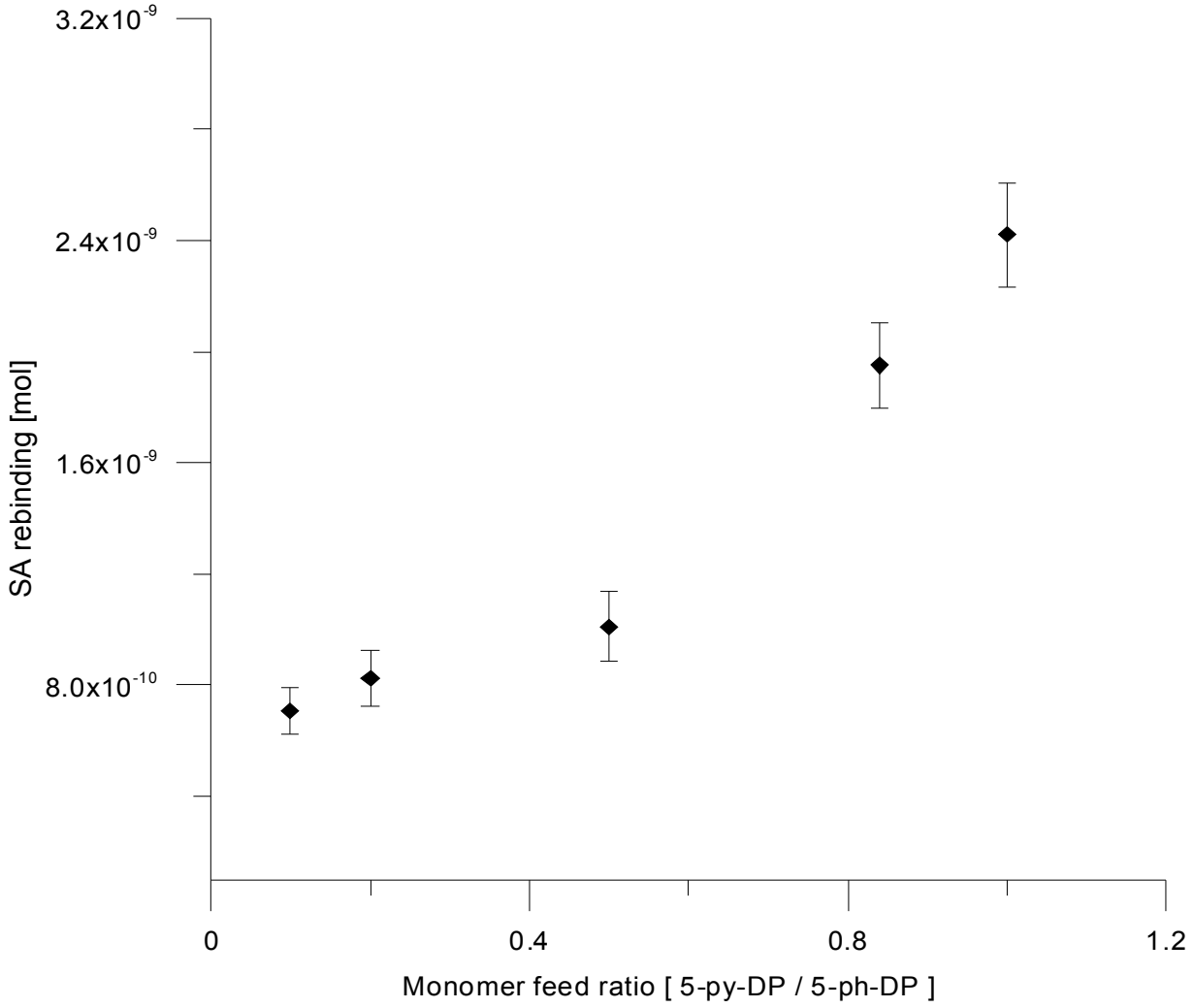

Figure 6: effect of the monomer feed ratio on the SA rebinding. All polymers obtained by cyclic voltammetry (17 cycles) at Pt-EQCM quartz crystal WE vs Ag/AgCl,Cl^-_{sat} in AN + 0.05 M TBAP.

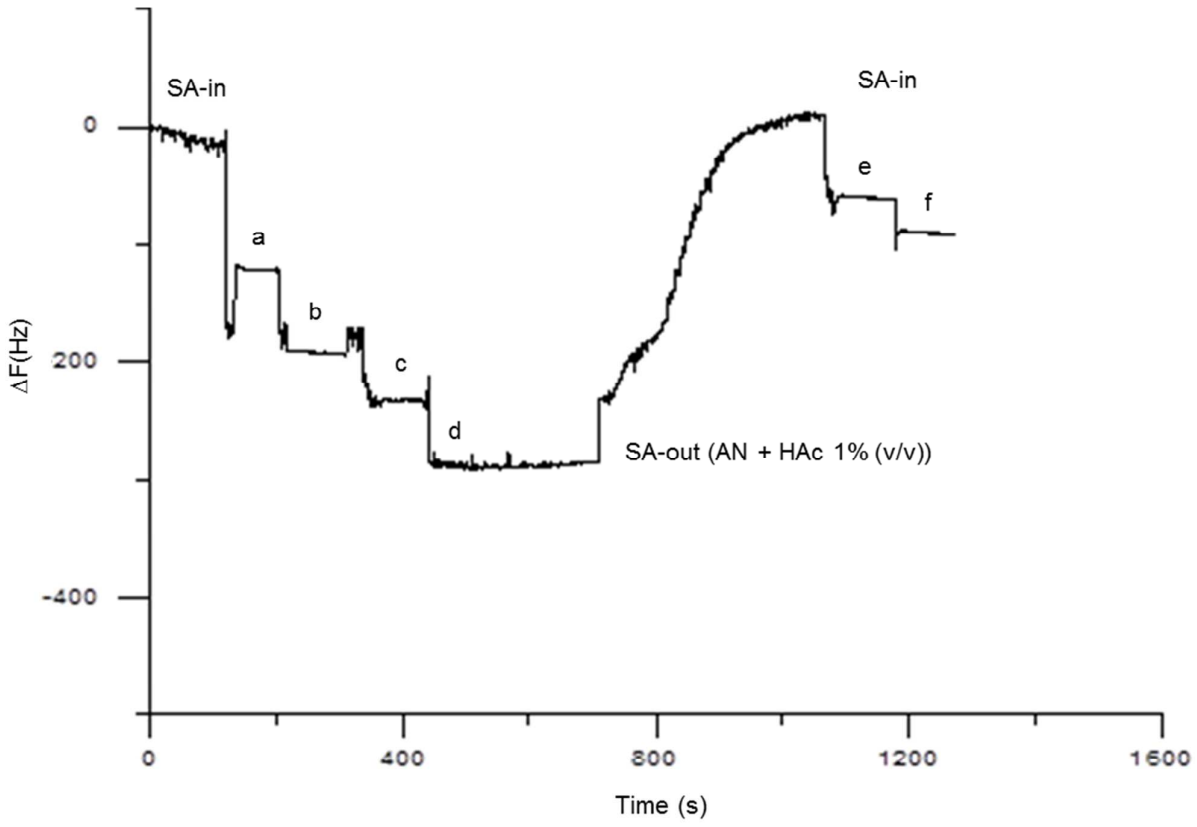

Figure 7: co-cMIP response at different total concentration of SA in solution: a) 1.5 10^{-7} M, b) 3.0 10^{-7} M, c) 4.5 10^{-7} M, d) 5.5 10^{-7} M, e) 0.7 10^{-7} M, f) 1.5 10^{-7} M.

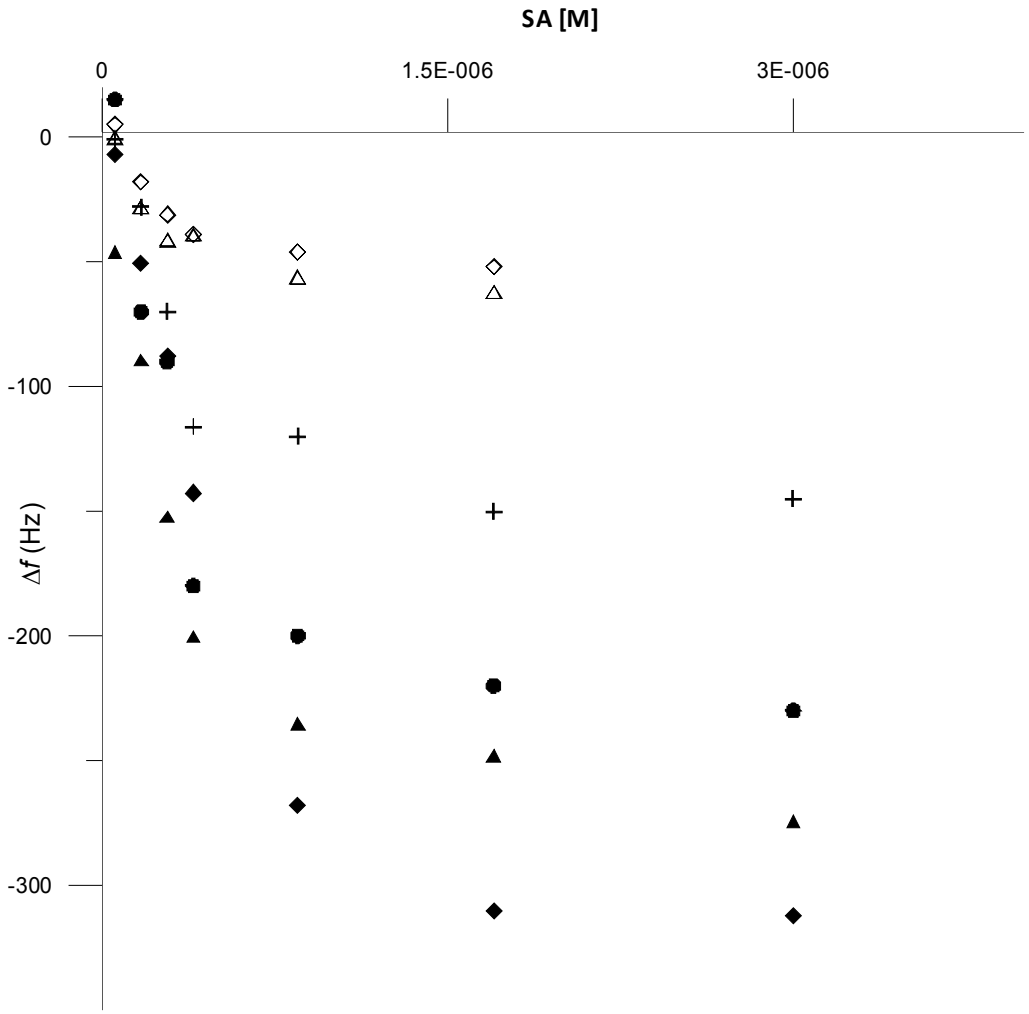

Figure 8: : QCM evaluation of SA-rebinding on (●) homo-poly-5-ph-DP c-MIP and (**+**) homo-poly-5-py-DP cMIP and their copolymer (▲) cMIP feed ratio 0.2: 0.6 mM 5-ph-DP + 0.12 mM 5-py-DP + 1.5 mM SA; (◆) cMIP feed ratio 1: 0.6 mM 5-ph-DP + 0.6 mM 5-py-DP + 1.5 mM SA; (△) cNIP feed ratio 0.2; (◇) cNIP feed ratio 1, prepared as cMIPs with no added template. All polymers obtained by cyclic voltammetry (17 cycles) at Pt-EQCM quartz crystal WE vs Ag/AgCl,Cl^-_{sat} in AN + 0.05 M TBAP.

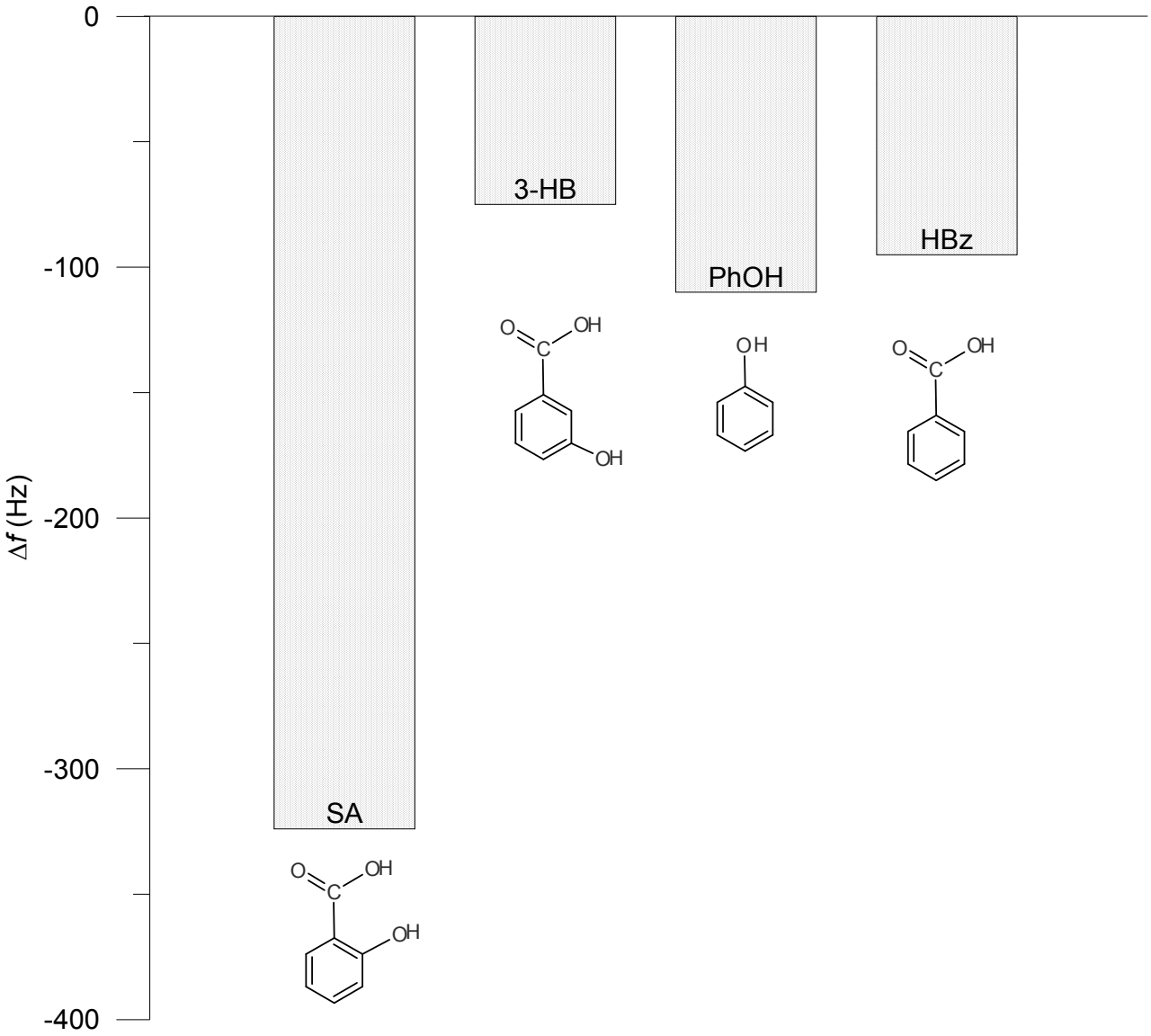

Figure 9: co-cMIP response as Δ*f*(Hz) due to SA and interferents molecules, 3-hydroxybenzoic acid (3-HB), phenol (PhOH) and benzoic acid (HBz). All species were 3 10^{-7} mol L^{-1} in AN + 0.05M TBAP.

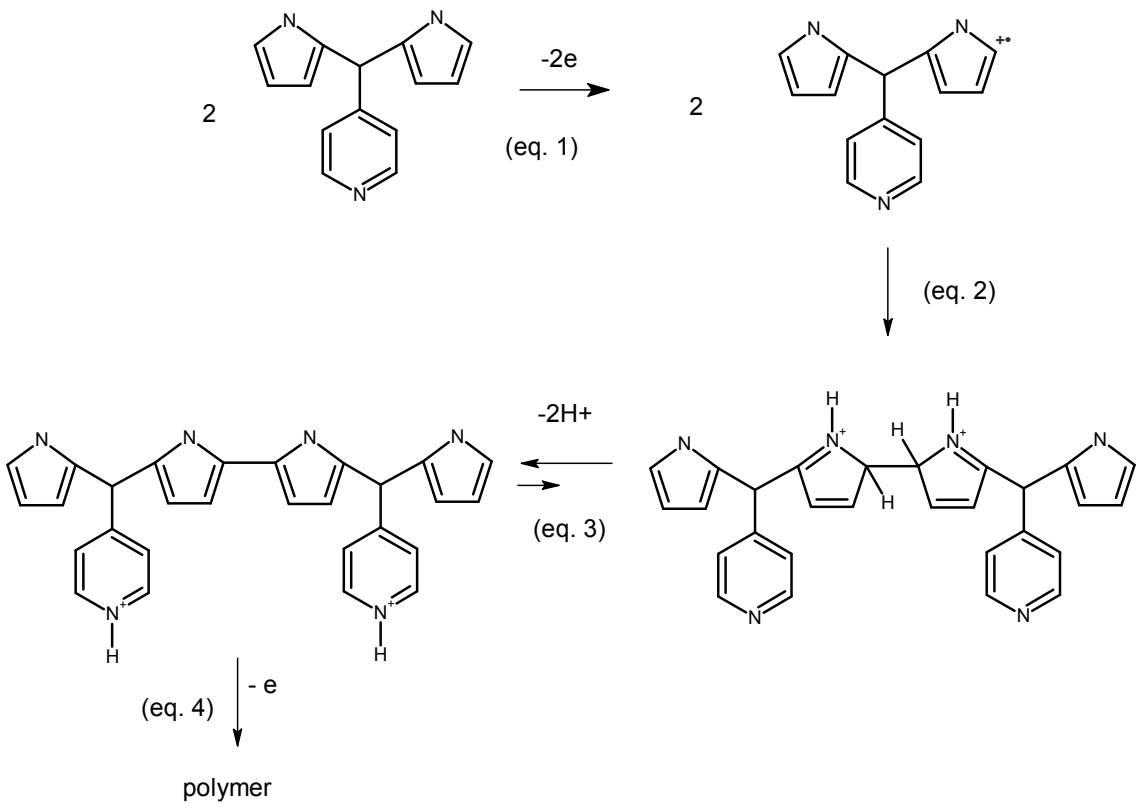

Scheme 1 : Proposed mechanism of the electrochemical oxidation of 5-py-DP

5-ph-DP			5-py-DP			Co-polymer 1:1		
Cycle number	cNIP[(1)] ng/cycle	cMIP [(2)] ng/cycle	Cycle number	cNIP[(3)] ng/cycle	cMIP[(4)] ng/cycle	Cycle number	cNIP[(5)] ng/cycle	cMIP[(6)] ng/cycle
1	58.96	109.21	1	53.6	80.4	1	187.6	250.58
2	168.84	178.622	2	53.6	67.0	2	235.84	320.26
3	188.94	206.896	3	40.2	60.3	3	235.84	301.5
4	182.24	223.78	4	33.5	46.9	4	233.16	294.8
5	198.32	230.48	5	26.8	40.2	5	235.84	296.14
6	188.94	257.28	6	13.4	26.8	6	231.82	298.82
7	195.64	280.06	7	13.4	26.8	7	235.84	301.5

Table 1: Example of the mass increase measured at each cycles of deposition of 5-ph-DP and 5-py-DP homo and co-polymers at Pt-quartz crystal. The reproducibility of the mass deposition of the films finally formed (CV%, n=10) was [(1)]3.5%, [(2)]7 %, [(3)]5.5 %, [(4)] 9 %, [(5)]5 %, [(6)]7.3 %.

5-py-DP (mM)	5-ph-DP (mM)	SA (mM)	Δf(Hz)
0.6	0	0	- 236.3 (± 4.0)
0	0.6	0	- 1045.2 (± 3.8)
0.6	0.6	0	- 1118.2 (± 5.6)
0.12	0.6	1.5	- 1293.3 (± 8.0)
0.3	0.6	1.5	- 1320.3 (± 5.2)
0.45	0.6	1.5	- 1423.8 (± 4.9)
0.6	0.6	1.5	- 1514.3 (± 5.4)
1.2	0.6	1.5	- 246.3 (± 6.5)

Table 2: Frequency shift (Hz) due to the copolymer deposition as co-cNIP and as co-cMIP at Pt-quartz crystal (17^{th} cycle)

Polymer composition([*])	Δf(Hz)/[SA](M)	CV% (n=3)	DL (3σ/S) (M)
[(*)]Salicylic acid concentration =1.5 mM			
5-py-DP	$-1.9\ 10^{+8}$	12%	$3.0\ 10^{-8}$
5-ph-DP	$-3.2\ 10^{+8}$	7.0%	$1.9\ 10^{-8}$
5-ph-DP 0.6 mM + 5-py-DP 0.12 mM	$-4.1\ 10^{+8}$	9.5%	$2.7\ 10^{-8}$
5-ph-DP 0.6 mM + 5-py-DP 0.6 mM	$-5.3\ 10^{+8}$	10%	$1.7_5\ 10^{-8}$

Table 3: SA sensitivity and detection limits for differently prepared cMIP.

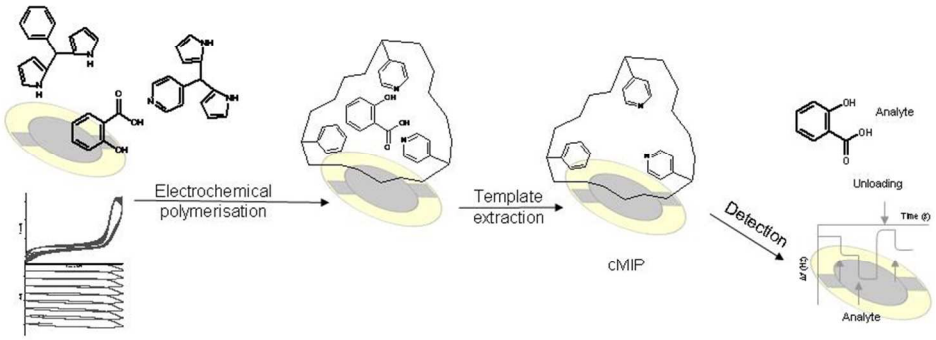

Graphical Abstract
254x190mm (96 x 96 DPI)